Supporting Information for

Perturbing Tandem Energy Transfer in Luminescent Heterobinuclear Lanthanide Coordination Polymer Nanoparticles Enables Real-Time Monitoring of Release of the Anthrax Biomarker from Bacterial Spores

Nan Gao,[†] Yunfang Zhang,[†] Pengcheng Huang,[*†] Zhehao Xiang,[†] Fang-Ying Wu,[*†] and Lanqun Mao[‡]

[†]College of Chemistry, Nanchang University, Nanchang 330031, China

[‡]Beijing National Laboratory for Molecular Sciences, Key Laboratory of Analytical Chemistry for Living Biosystems, Institute of Chemistry, the Chinese Academy of Sciences, Beijing 100190, China

*E-mails: Pengcheng Huang, pchuang@ncu.edu.cn; Fangying Wu, fywu@ncu.edu.cn. Tel/Fax: 011-86 79183969882.

Table of Contents

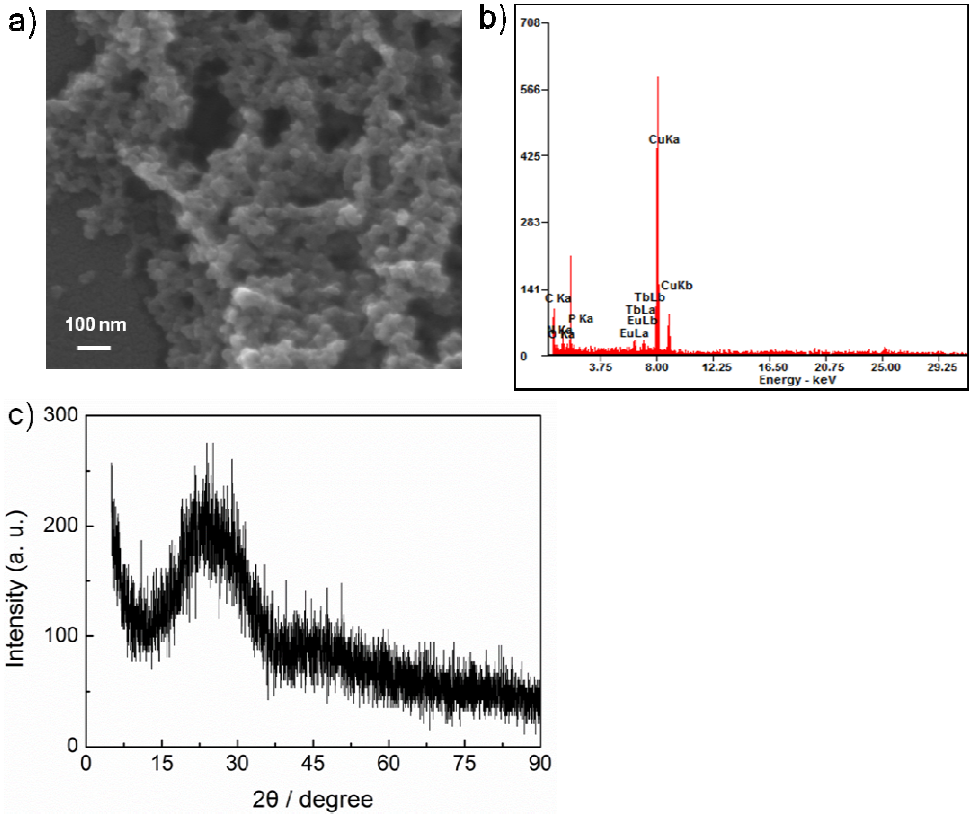

Figure S1. (a) SEM image, (b) EDX data, and (c) PXRD pattern of GMP-Tb/Eu. Note that the diffraction peak at ca. 22.5° arose from the sample stage-the glass substrate.

Table S1. The ICP-MS analysis results of as-prepared GMP-Tb/Eu upon addtion of DPA (0, 100 and 600 μM).

Sample	Measured concentration (mg/L)		n_{Tb}:n_{Eu}
	Eu	Tb	
1	0.45	2.2	4.7
2	2.1	10	4.6
3	4.2	22	5.0

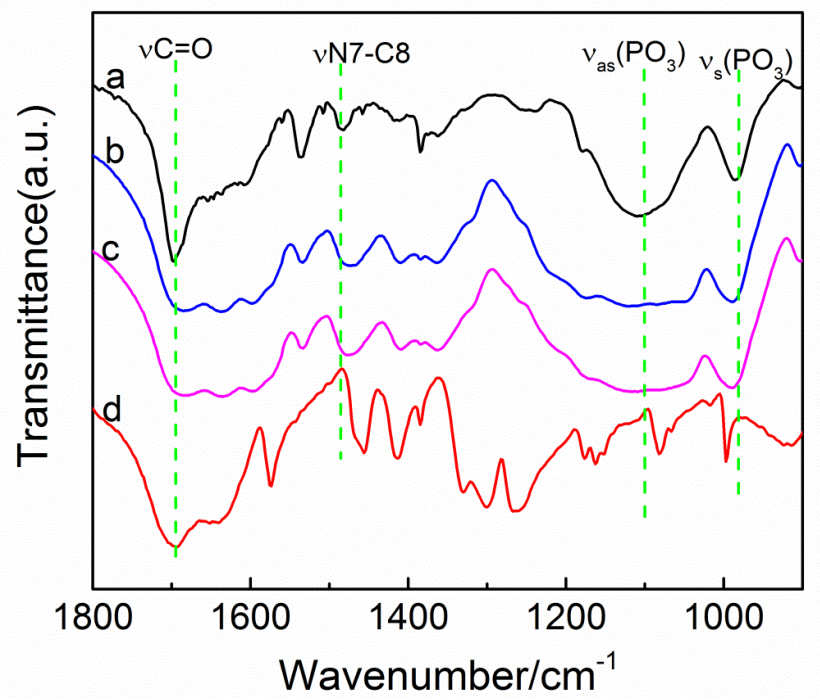

Figure S2. FTIR spectra of GMP (a), DPA (d), and GMP-Tb/Eu in the absence (b) and presence (c) of DPA.

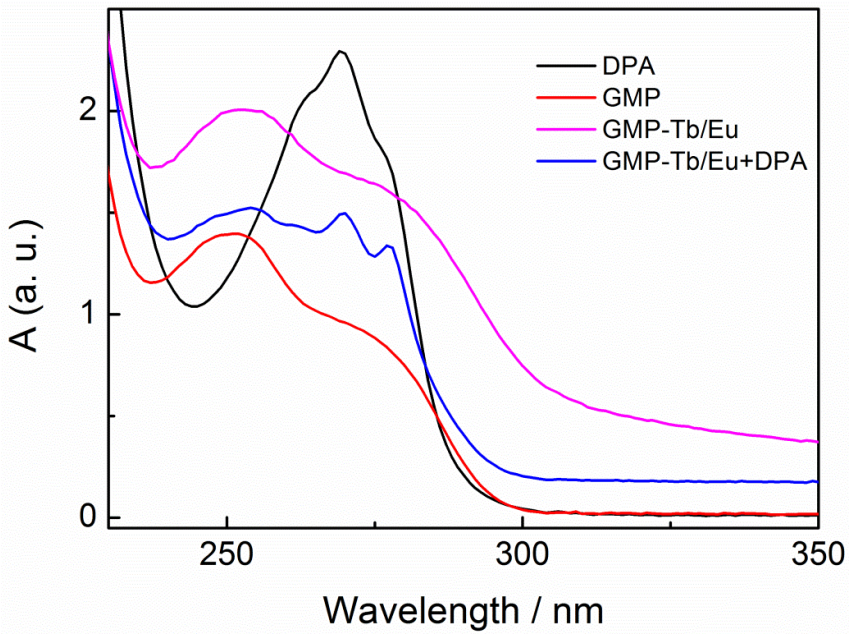

Figure S3. UV−vis absorption spectra of GMP, DPA, and GMP-Tb/Eu in the absence and presence of DPA.

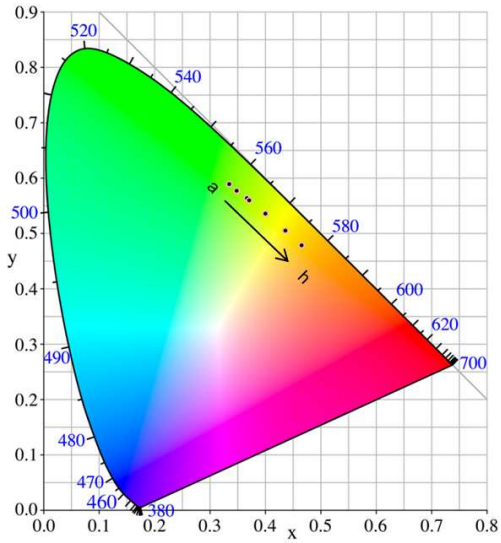

Figure S4. CIE coordinates of GMP-Tb/Eu with various Tb^{3+}/Eu^{3+} ratios (a→h: 1:0, 100:1, 50:1, 30:1, 10:1, 8:1, 5:1, 4:1).

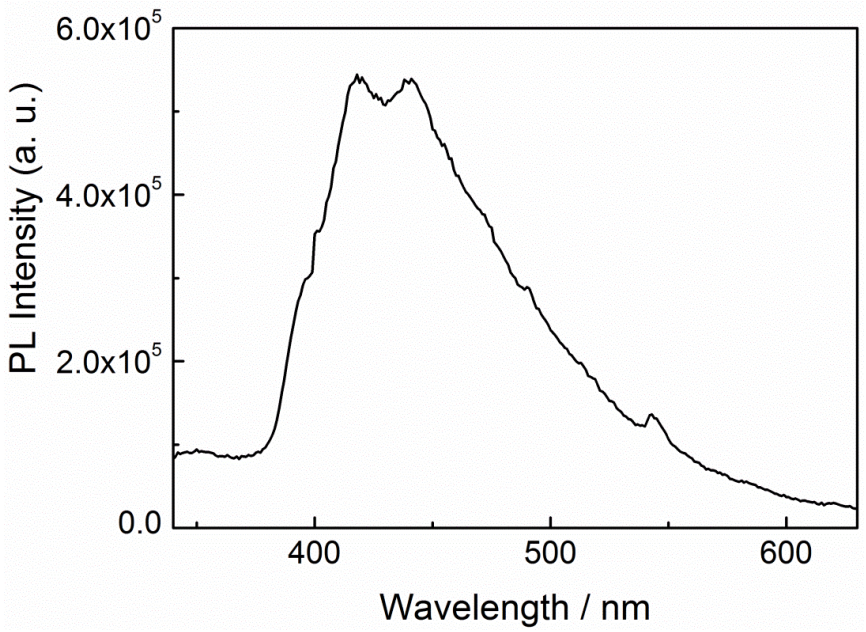

Figure S5. Phosphorescence spectrum of GMP-Gd at 77 K.

Because the $^6P_{7/2} \rightarrow {}^8S_{7/2}$ Gd^{3+} transition occurs at high energy (ca. 32000 cm^{-1}), the observed peak

is ascribed to a triplet ligand emission.[1]

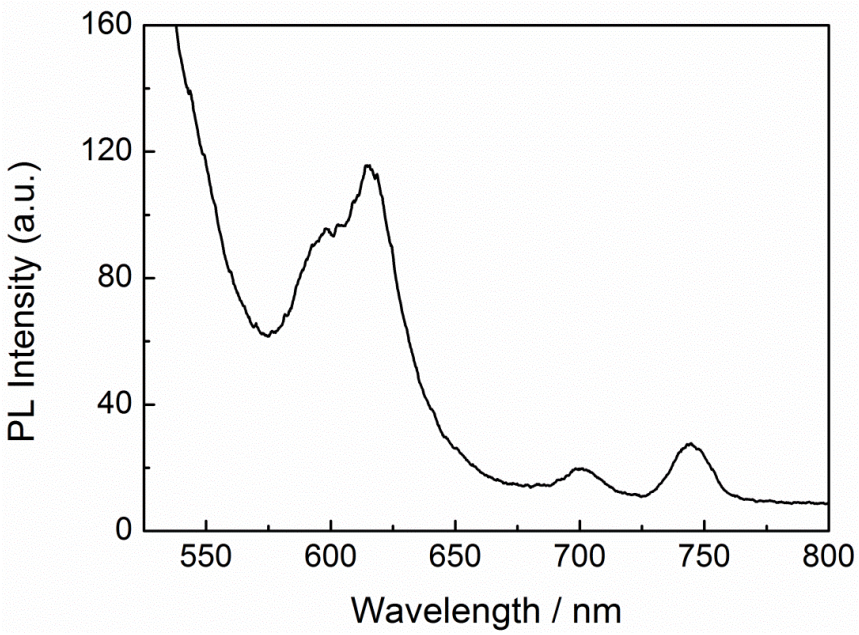

Figure S6. Emission spectrum of GMP-Tb/Eu excited with 494 nm.

Table S2. The $^5D_4$ of Tb^{3+} and $^5D_0$ of Eu^{3+} lifetimes and the efficiency (η) of this intermetallic energy transfer from Tb^{3+} to Eu^{3+} for a series of GMP-Tb/Eu with different Tb^{3+}/Eu^{3+} ratios. The decay curves are monitored at 544 nm and 614 nm, respectively.

$n_{Tb}:n_{Eu}$	τ_{Tb} (ms)	τ_{Eu} (ms)	η
1:0	1.070	-	-
10:1	0.632	0.560	0.41
5:1	0.567	0.494	0.47
1:1	0.429	0.352	0.60
1:5	0.408	0.280	0.62
0:1	-	0.242	-

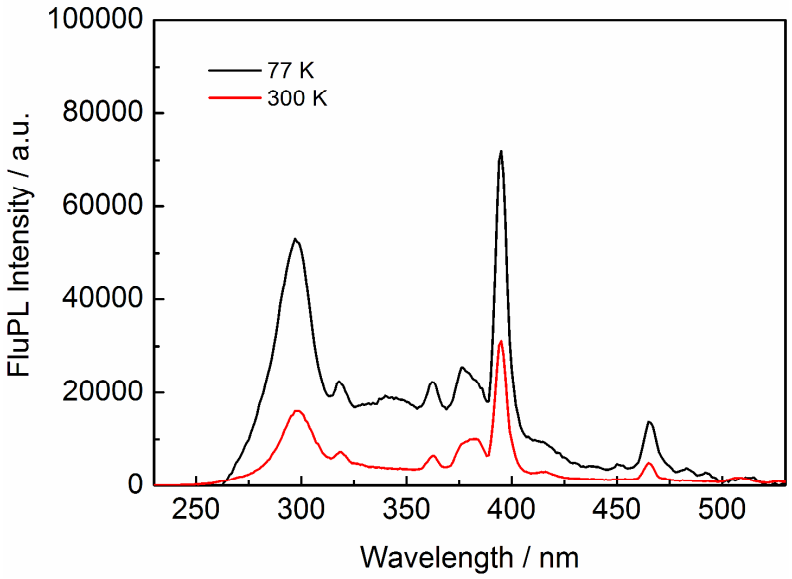

Figure S7. Excitation spectra of GMP-Tb/Eu recorded at room temperature and at 77 K.

The excitation spectrum at room temperature did not present any band of the ligand GMP that

could suggest the presence of an antenna effect. This excitation spectrum thus supports the existence of a photo-induced electron transfer (PET) mechanism for GMP-Tb/Eu especially when the Tb^{3+}/Eu^{3+} ratio was very low.[2,3] On the other hand, the PET mechanism is supposed to o become less efficient when the temperature is lowered, which was observed for GMP-Tb/Eu at 77 K.[2,3]

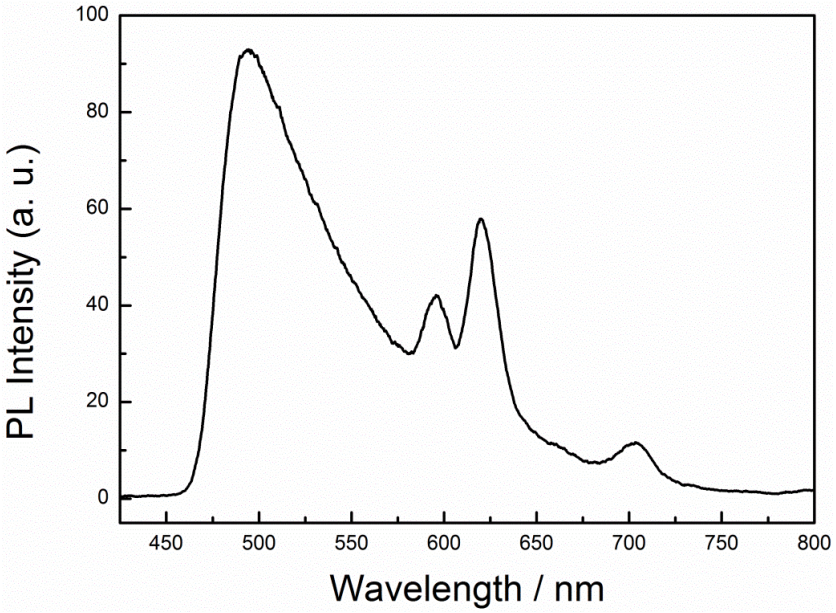

Figure S8. Emission spectrum of GMP-Tb/Eu excited with 395 nm.

This excitation wavelength of 395 nm is a wavelength that corresponds to a direct excitation of the Eu^{3+} ion ($^7F_0 \rightarrow {}^5D_3$ transition). This spectrum further confirmed that the PET mechanism was present and that back transfer is not responsible for the absence of luminescence.[2,3]

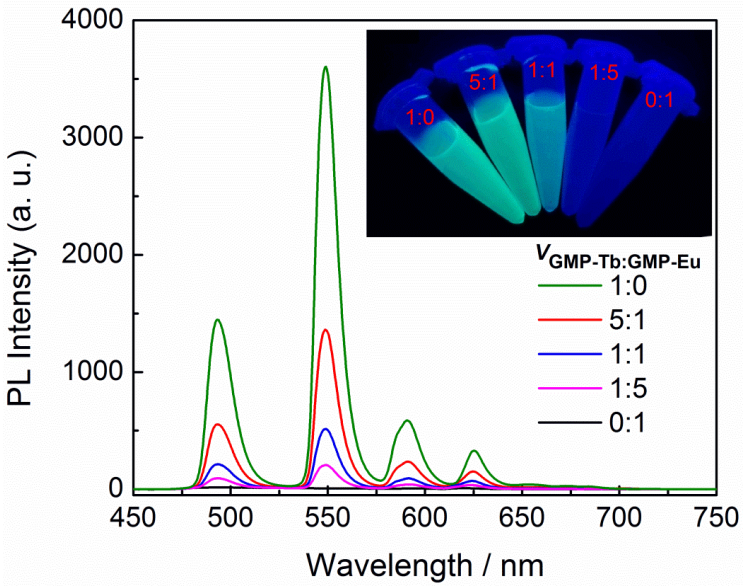

Figure S9. Emission spectra of the mixtures of GMP-Tb and GMP-Eu suspensions at different volume ratios with different volume ratios of Eu^{3+}/Tb^{3+} and the corresponding luminescence photograph.

It was found that the cocktail only emited green luminescence although the emission intensities declined sharply as the amount of GMP-Tb decreased, which supported that GMP cannot sensitize Eu^{3+} luminescence and GMP-Eu did not accept the excited energy of GMP-Tb. This also indirectly confirmed the absence of the intermolecular energy transfer between GMP-Tb and GMP-Eu and the homogeneity of the heterobinuclear Ln-CPNs GMP-Tb/Eu.

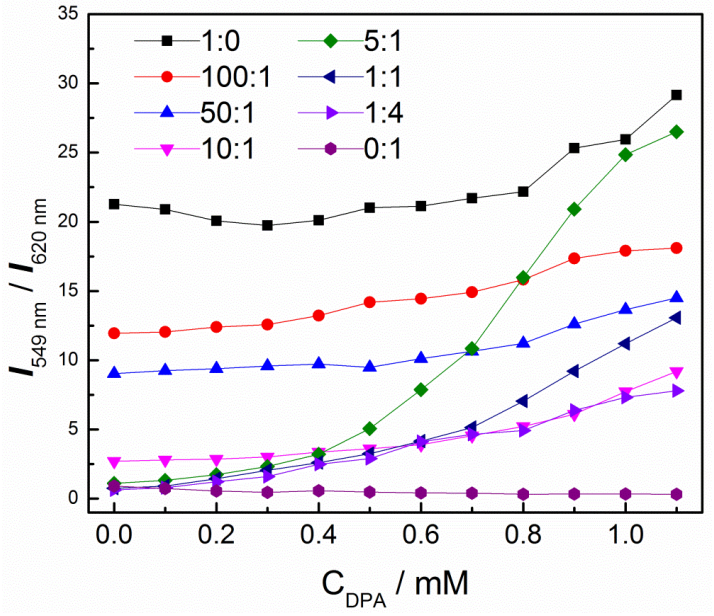

Figure S10. The relative emission intensity (I_{549}/I_{620}) of GMP-Tb/Eu with various Eu^{3+}/Tb^{3+} ratios at different concentrations of DPA.

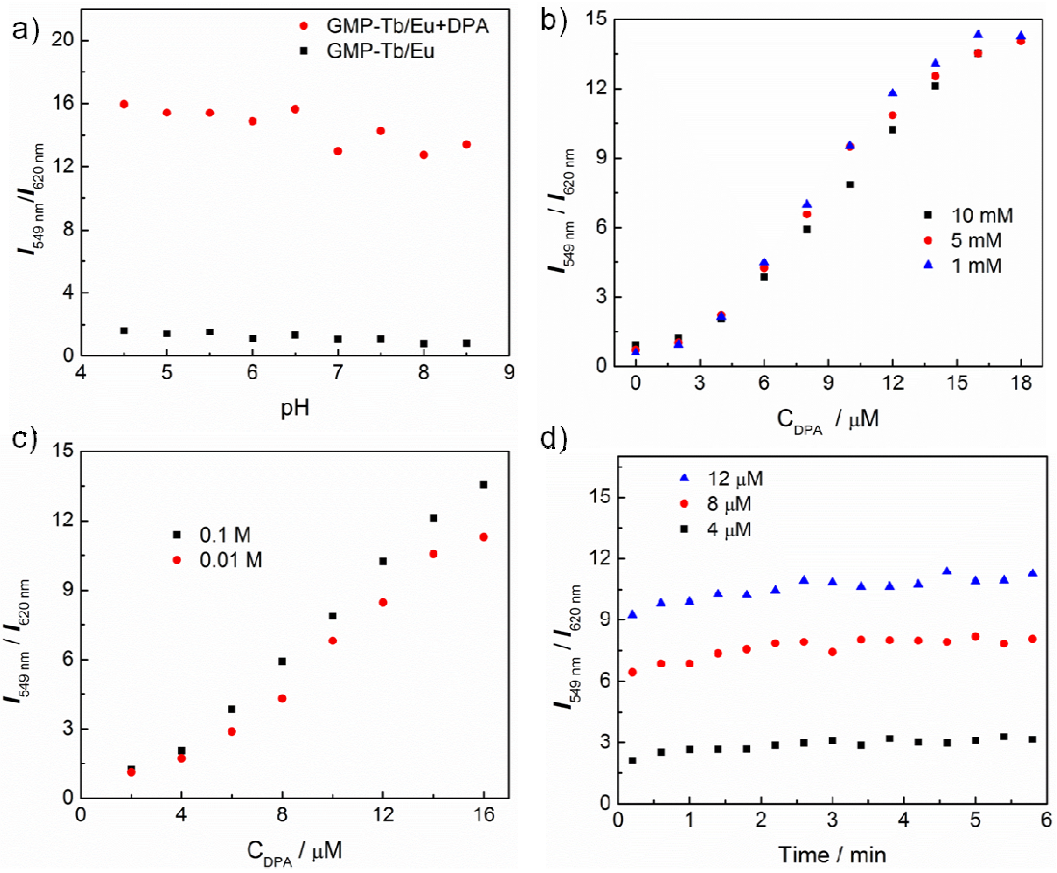

Figure S11. (a) The pH effect on the luminescent repsonse of GMP-Tb/Eu toward DPA (16 μM). (b), (c) Effects of the variation in concentration of initial solutions during the preparation of the sensor GMP-Tb/Eu, or in the concentration of buffer solution on the luminescent repsonse of GMP-Tb/Eu toward different concentrations of DPA. (d) The temporal profiles of relative emission intensity (I_{549}/I_{620}) of GMP-Tb/Eu in the presence of different concentrations of DPA.

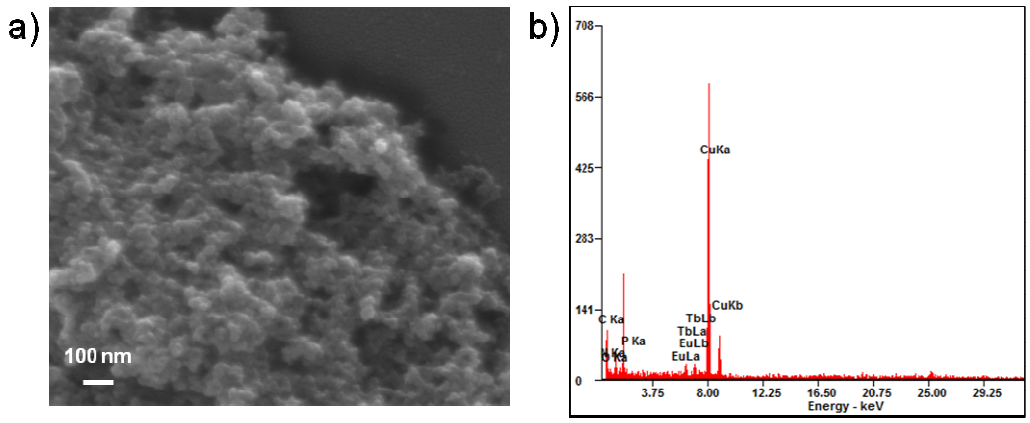

Figure S12. (a) SEM image, and (b) EDX data of GMP-Tb/Eu upon addition of DPA.

In Image a, it can be seen that the introduction of DPA did not have an obvious effect on the morphology and size of GMP-Tb/Eu, implying the structural integrity. The corresponding EDX analysis (Image b) revealed that the content of N element increased (from 17.1% to 21.5%), suggesting the formation of an adduct of DPA and GMP-Tb/Eu.

Table S3. The $^5D_4$ of Tb^{3+} and $^5D_0$ of Eu^{3+} lifetimes and the efficiency of this intermetallic energy transfer (η) from Tb^{3+} to Eu^{3+} for GMP-Tb/Eu upon addtion of DPA (0, 25 and 50 μM).

C_{DPA} (μM)	τ_{Tb} (ms)	τ_{Eu} (ms)	η
0	0.567	0.494	0.47
25	0.782	0.471	0.27
50	1.030	0.443	0.04

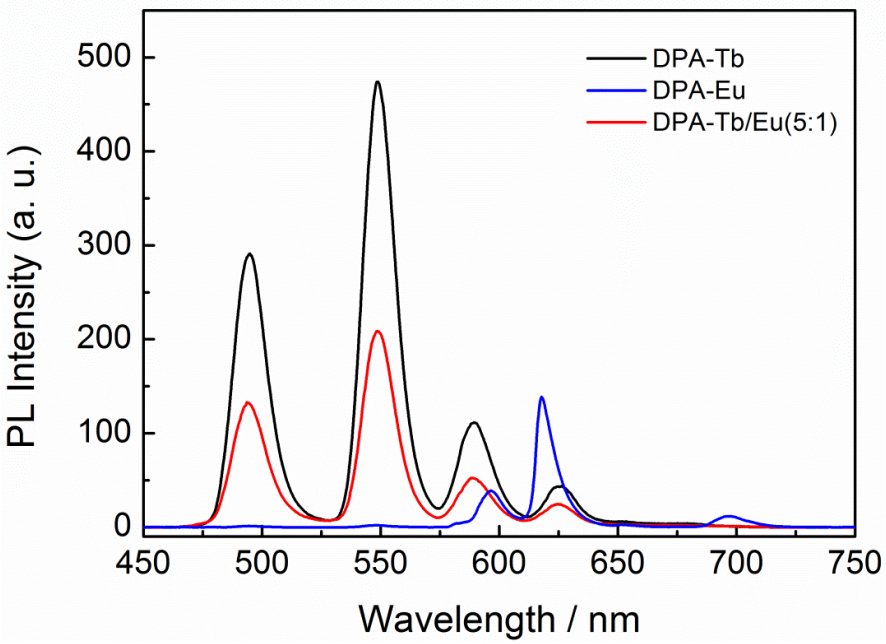

Figure S13. Emission spectra of the mixtures of DPA + Tb^{3+}, DPA + Eu^{3+}, and DPA + Tb^{3+}/Eu^{3+} (n_{Tb}:n_{Eu} = 5:1). For the three, the concentration of DPA is the same as the total concentration of lanthanide ions.

In this figure, it can be seen that under the same conditions, the luminescence intensity of the complex DPA-Tb at 549 nm was much stronger than that of the complex DPA-Eu at 620 nm. This showed that Tb^{3+} has a more sensitive and intense luminescence response upon coordination with DPA than Eu^{3+} at a given DPA concentration and excitation intensity, which confirmed the higher binding ability of DPA with Tb^{3+} than Eu^{3+}. Furthermore, the ternary complex DPA-Tb/Eu with a Tb^{3+}/Eu^{3+} ratio of 5:1 exhibited a similar emission spectrum to the complex DPA-Tb, also supporting the above conclusion. Note that weaker luminescence intensity than the complex DPA-Tb was mainly because of Eu^{3+} doping.

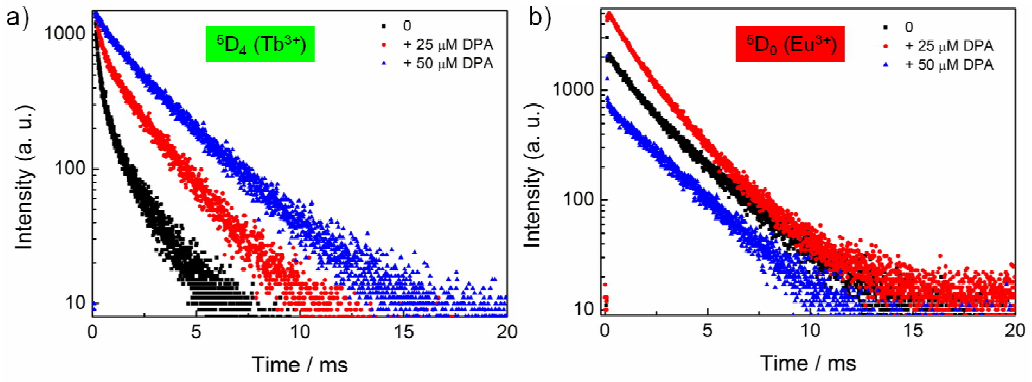

Figure S14. Decay curves of (a) $^5D_4$ (Tb^{3+}) and (b) $^5D_0$ (Eu^{3+}) lifetimes of GMP-Tb/Eu upon addition of different concentrations of DPA in D_2O, respectively.

Table S4. The $^5D_4$ of Tb^{3+} and $^5D_0$ of Eu^{3+} lifetimes in D_2O and the average number (q) of coordinated water molecules in the coordination sphere of Eu^{3+} and Tb^{3+} upon addition of different concentrations of DPA (0, 25 and 50 μM).

C_{DPA} (μM)	τ_{Tb} (ms)	q_{Tb}	τ_{Eu} (ms)	q_{Eu}
0	1.245	1.013	2.740	1.747
25	2.060	0.833	2.299	1.774
50	2.480	0.595	1.864	1.808

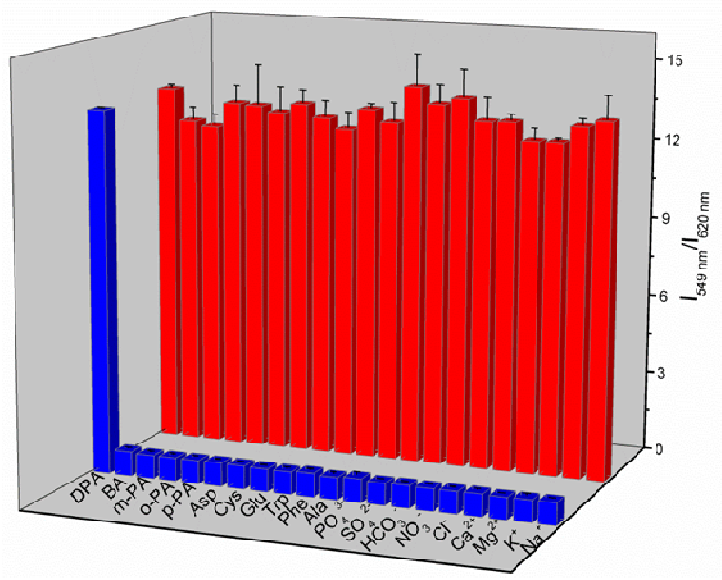

Figure S15. Selectivity (blue bar) and competition experiments (red bar) of GMP-Tb/Eu for DPA over several aromatic ligands, amino acids, metal ions, and anions. All the measurements were acquired under identical conditions. The concentration of DPA is 16 μM. The concentrations of K^+, Na^+, Mg^{2+}, NO_3^-, HCO_3^-, SO_4^{2-}, and Cl^- are all 16 mM, those of Ala, Phe, and Cys are 1.6 mM, Trp, Glu, Asp, and BA are 160 μM, and Ca^{2+} and PO_4^{3-} are 80 μM, and p-PA, o-PA, and m-PA are 16 μM.

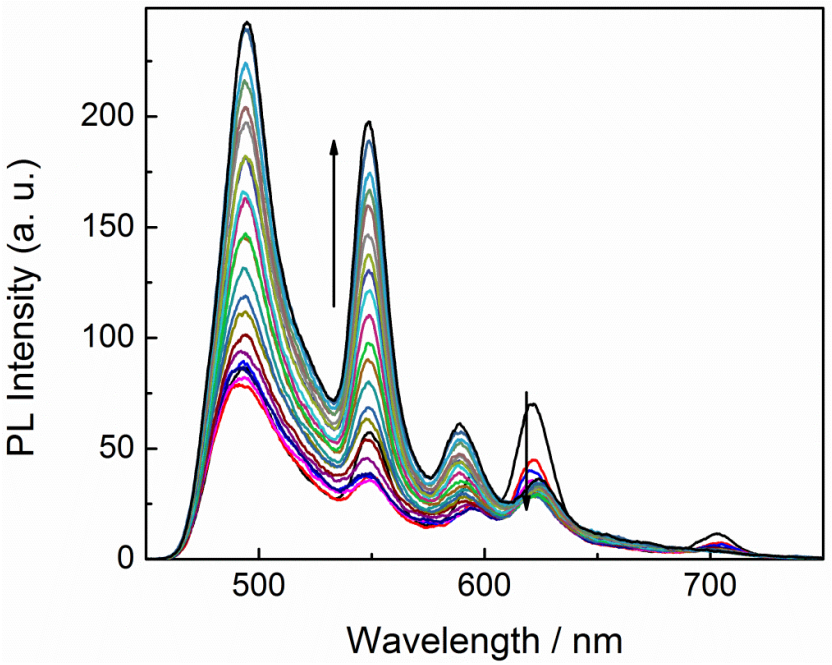

Figure S16. Emission spectra of GMP-Tb/Eu by successive addition of the filtrate (5 μL) of the suspension of bacterial spores after the germination process triggered by alanine at 70 °C for 60 min.

References

(1) Zhou, J. M.; Li, H. H.; Zhang, H.; Li, H. M.; Shi, W.; Cheng, P. *Adv. Mater.* **2015**, 27, 7072 – 7077.

(2) Fan, X.; Freslon, S.; Daiguebonne, C.; Calvez, G.; Le Pollès, L.; Bernot, K.; Guillou, O. *J. Mater. Chem. C* **2014**, 2, 5510 – 5525.

(3) Freslon, S.; Luo, Y.; Calvez, G.; Daiguebonne, C.; Guillou, O.; Bernot, K.; Michel, V.; Fan, X. *Inorg. Chem.* **2014**, 53, 1217 − 1228.